Transmission line torsional stiffness. Confrontation of field-tests line and finite element simulations.

Renaud Keutgen and **Jean-Louis Lilien**
Montefiore Electrical Institute
University of Liège, B-4000 Liège, Belgium

Teruhiro Yukino
Kansai Electric Power Co, Osaka, Japan

Abstract - Exceptional full-scale field-tests on a quad bundle line were led by KANSAI EPCO. These tests, which were performed in 1995, measured the torsional stiffness on a long dead-end span ($\cong$ 640m). This paper gives a description of the tests and their results as well as a confrontation with finite element simulations. A comparison is also performed with other existing simplified methods. Basic parameters of bundle torsional stiffness are clearly pointed out.

I. INTRODUCTION

Overhead transmission lines are characterised by a highly flexible form. This fact leads to frequent dynamical interactions between the line and external loads like wind and ice.

The study of these phenomena requires a good knowledge of the stiffness terms coupled with the different movements and in particular the torsional stiffness of the line.

When the torsional stiffness of single conductors is linear and depends only on the size, the construction and the age of the conductors, bundle torsional stiffness is mainly non-linear and depends on many design parameters like the sag/span ratio, the disposition of the spacers, the geometry of the bundle and the attachments to anchoring towers by the use of yoke plates.

Experimentally, the complexity of the bundle torsional stiffness can be analysed by applying a torque on the line at a spacer location to assess the rotation angle in the same place.

h full-scale field-tests were performed on a quad bundle by KANSAI EPCO.

The obtained results during this campaign of tests are very interesting because many parameters were involved (no level span, no regular spacer location, different design of yoke plates, initial tension differences between upper and lower subconductors) and measured (spacer rotation, rotation of the yoke plates, variation of the tension in all subconductors) so that the confrontation with different models can enlighten their limitations.

PE-247-PWRD-0-12-1997 A paper recommended and approved by the IEEE Transmission and Distribution Committee of the IEEE Power Engineering Society for publication in the IEEE Transactions on Power Delivery. Manuscript submitted July 28, 1997; made available for printing December 12, 1997.

Based on these exceptional full-scale field-results, the paper tries to underscore the most significant design parameters for the bundle torsional stiffness.

To reach this goal, we first remind the reader of the main existing simplified theories concerning the bundle torsional stiffness.

Then a description of the tests led by KANSAI EPCO on a dead-end span quad bundle is given.

The experimental results are next compared with the existing simplified methods, and point out the limitation of their hypotheses.

Then a finite element model is presented and again confronted with the field results. This model allows to better understand the role of certain design parameters like the sag/span ratio, the disposition of the spacers, the geometry of the bundle and the attachments to anchoring towers by the use of yoke plates.

Finally, by way of conclusion, the basic parameters of the torsional stiffness are reviewed and the application limit of each simplified theory is detailed.

II. STATE-OF-THE-ART

A. Description of the problem

As it is mentioned before, the bundle torsional stiffness can be studied thanks to a torque/rotation angle diagram (Fig. 1).

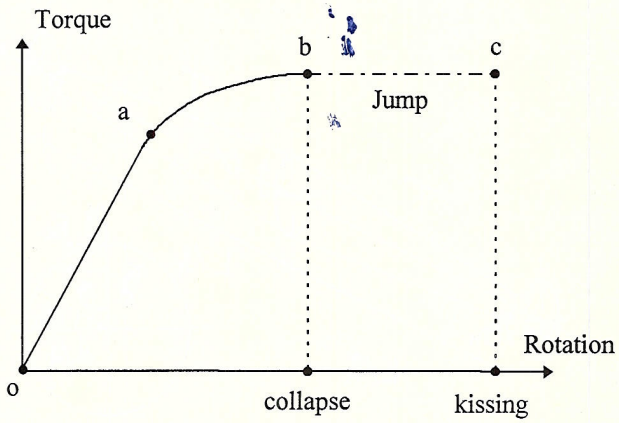

Fig. 1. Torque/rotation angle diagram.

This kind of curve can be obtained experimentally but also with a theoretical model. The comparison between the two approaches allows then to assess the validity of the hypotheses assumed in the theoretical representation.

Physically the torsional stiffness is calculated by differentiating the torque with respect to the angle of rotation. For bundle conductors, the torque/rotation angle relation can

be divided into two parts until the collapse, respectively the linear part (oa on Fig. 1) and the non-linear part (ab on Fig. 1). Strictly speaking, it means that for the non-linear part, we are dealing with a tangent torsional stiffness.

The collapse condition, which is identified by the collapse angle on Fig. 1, is fulfilled when the applied torque exceeds a critical value. At this moment, the bundle rotation grows so large that the subconductors of two subspans (one on each side from the place where the torque is applied) touch each other. This contact is called "kissing" and is characterised by the kissing angle.

All these properties of the torque/rotation angle relationship are highly determined by design parameters like the sag/span ratio, the disposition of the spacers, the geometry of the bundle and the attachments to anchoring towers by the use of yoke plates.

B. Nigol's theory [1, 2, 3]

In 1977, Nigol and Clarke [1] presented a complete model for bundle torsional stiffness. In this work, the expression for the torsional moment is obtained for a symmetrical arrangement of the bundle for which the torque is applied at the centre of the span and for which equal length of the subspans are considered.

Further hypotheses are assumed such as :

1. the sag is neglected in relation to the span length
2. the radius of the bundle all along the subspan is supposed to remain constant during the torsion of the latter
3. the tension in each subconductor is equal and remains constant during the torsion of the bundle

Knowing this, the torsional moment on the central spacer is assessed, with the help of Fig. 2, by considering the reaction forces in the x and y directions and their respective moment around the centre of the bundle.

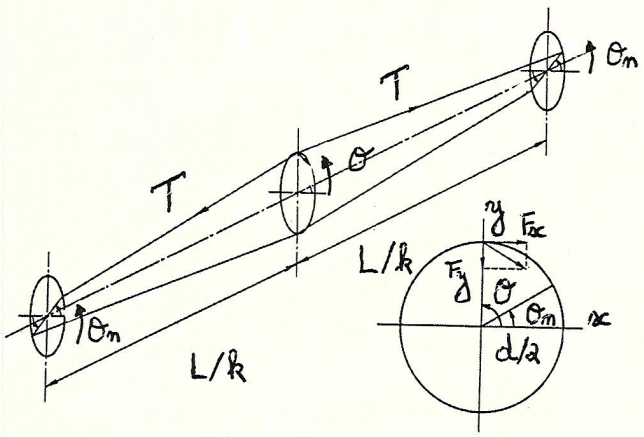

Fig. 2. Forces and moments acting on bundle conductors with more than one spacer per span [1].

This leads to the following formulas for n subconductors :

$$F_x = \frac{Tdk}{L}\left(\cos\theta_n - \cos\theta\right)$$
$$F_y = \frac{Tdk}{L}\left(\sin\theta - \sin\theta_n\right) \quad (1)$$

and,

$$\Rightarrow M = n\left(F_x \frac{d}{2}\sin\theta + F_y \frac{d}{2}\cos\theta\right)$$
$$= \frac{nTd^2k}{2L}\sin\left(\theta - \theta_n\right) \quad (2)$$

L = total length of the span.
n = number of subconductors.
T = initial tension in each subconductor.
d = diameter of the bundle.
k = number of subspans.
θ = torsional rotation where the torque is applied.
θ_n = torsional rotation one spacer before the place where the torque is applied.

The final result has also to take into account the intrinsic torsional stiffness of each subconductor, so that Nigol finally writes :

$$M = \frac{nTd^2k}{2L}\sin\left(\theta - \theta_n\right) + \frac{2nsk}{L}\left(\theta - \theta_n\right) \quad (3)$$

s = intrinsic torsional stiffness of each subconductor

A last assumption has to be made concerning θ_n in (3) in order to use this one. For $\theta \le \frac{\pi}{4}$, the torsion along the span can be approached by a linear behaviour, so that θ_n is given by :

$$\theta_n = \frac{k-2}{k}\theta \quad (4)$$

and the torsional moment by :

$$M = \frac{nTd^2k}{2L}\sin\left(\frac{2\theta}{k}\right) + \frac{4ns\theta}{L} \quad (5)$$

All these developments lead to the conclusion that Nigol's theory is only valid for small torsional movements and also, as we will see later, for subconductors in which the tension can be assumed to be constant during the torsional deformation of the bundle, even for small rotations.

C. Design of yoke plates

Recently, J. Wang [5] developed a new 3-DOF model to study galloping of single and bundle conductors. In this theory, a particular attention is paid to the physical mechanism of bundle torsional stiffness.

The same kind of reasoning is followed to tackle the description of the torsional moment which is also assessed by considering the reaction forces in the x and y directions and their respective moment around the centre of the bundle at the spacer where the torque is applied.

However, some side effects such as the attachments to anchoring by the use of yoke plates and on the other hand some effects inside the span such as the sag/span ratio and the

radius of the bundle during the torsional deformation are carefully examined.

The description of the role of the yoke plate design in the physical mechanism of bundle torsional stiffness is the major contribution of J. Wang's work. In this new theory, the subconductor tension is not constant during the torsional deformation of the bundle. It is given by :

$$T_i = \frac{T_0}{n} + \Delta T_i \qquad (6)$$

where T_0 is the initial tension of the bundle, n is the number of subconductors and ΔT_i is the tension variation in the subconductor i of the section. This tension variation in each subconductor is in relation with the design of the yoke plates.

Generally, this relation can be expressed according to one parameter h, which is the yoke plate dimension. Two extreme cases have to be considered for h, respectively $h = 0$ and $h = \infty$ (Fig. 4).

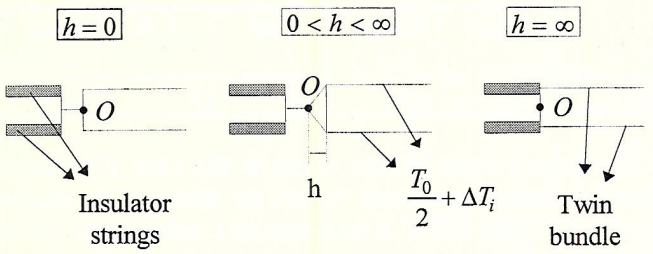

Fig. 4. Upper view of the yoke plate arrangement for an horizontal twin bundle.

If bundle rotation occurs, when $h = 0$, the ΔT_i remain null because the rotation around point O is free. This case corresponds to Nigol's theory. When $h = \infty$, the ΔT_i are the biggest because there is no possible rotation around O.

It must be noticed that, even if the tension variations between subconductors are small, they can increase the bundle stiffness by more than 50% for a dead-end span.

D. Finite element method

The finite element method can also be used to evaluate the torque/rotation angle relationship. The major advantage of finite elements lies in the discretisation of the problem. They allow to take into account very specific aspects of the transmission line.

The quad bundle tested at the KANSAI EPCO exhibits several particular aspects which render the finite element method particularly appropriate to the study of this problem.

Indeed we can already observe four characteristics of this quad bundle for which the hypotheses of the simplified methods are not fulfilled :

1. the span is unlevelled
2. there is a difference of initial tension between the two upper subconductors and the two lower subconductors
3. the length of the subspans are irregular
4. the design of the yoke plates can not be represented with only one design parameter h as it can in J. Wang's model. Moreover, several configurations of the yoke attachment were tested.

All these points were carefully described by the finite element model used in this paper.

III. DESCRIPTION OF THE FIELD-TESTS

A. Structure

The dead-end span quad bundle is 640 meters long and there is a difference of level of 120 meters between the two anchoring points.

The arrangement of the bundle is so that we have two upper subconductors and two lower subconductors.

The span is equipped with 14 spacers. Each of them weights 14 kilos. Their position along the span is given in Table 1.

TABLE 1. POSITION OF THE SPACERS ALONG THE SPAN.

Spacer number	**1**	**2**	**3**	**4**	**5**	**6**	**7**
Distance from the	35	75	120	170	225	265	305
forward anchoring (m)	345	385	425	480	530	575	615
Spacer number	**8**	**9**	**10**	**11**	**12**	**13**	**14**

The forward anchoring is made of an assembly of insulators and yoke plates. For this anchoring, between the yoke plates, a rod and a fixing plate were installed and then removed to change the assemblies conditions. More details concerning these asemblies conditions of the forward anchoring are given in section V.

The assembly of the backward anchoring is without insulators and the conditions are not changed.

B. Cables

The kind of used conductors is TACSR. The characteristics of the conductors are shown in Table 2.

TABLE 2. CHARACTERISTICS OF THE CONDUCTORS.

Item	*Unit*	*Value*
Diameter	*mm*	38.4
Cross section area	mm^2	870.8
Young modulus	N/m^2	$7.1\ 10^{10}$
Unit weight	kg/m	2.7
Number of strand	*Al/St*	45/7
Intrinsic torsional stiffness	Nm^2/rad	600

C. Tests

In order to apply a torque on the bundle, one extra spacer is used. This spacer is equipped with a potentiometer that allows to measure the rotation angle.

According to the assemblies conditions of the forward anchoring and to the initial sagging tension in the different subconductors (upper and lower subconductors), three experimental cases were managed. The Table 3 summaries the conditions for each case.

TABLE 3. CONDITIONS IN EACH TESTED CASE.

	Mean tension	*Upper tensions*	*Lower tensions*
Case1	37700 N	40200 N	35200 N
Case2	48650 N	53000 N	44300 N
Case3	46650 N	50100 N	43200 N
Case3	Removed		Free
Case2	Installed		Fixed
Case1	Installed		Fixed
	Rod and fixing plate		*Assembly*

In each case, the torque was applied at 50 and 100 meters far from the forward anchoring. In case1, the torque was also applied at 200 meters far from the forward anchoring.

IV. COMPARISON BETWEEN FIELD RESULTS AND SIMPLIFIED METHODS

A. Introduction

The simplified methods can only be used for a torque which is applied at mid-span. The nearest case for this situation led at the KANSAI EPCO is the one where the torque was applied at 200 meters from the tower (case1_200m) so that the comparison will be led with this case.

We have also to keep in mind that for the simplified methods the span is level, the subspan lengths are equal and there is no difference of initial tension between the two upper and the two lower subconductors. The initial tension in each subconductor is equal at the mean initial tension of all subconductors of the experimental line, namely 37700N.

Concerning J. Wang's method, the two extreme cases for the design of the yoke plates, respectively $h = 0$ and $h = \infty$ are simulated.

B. Comparison

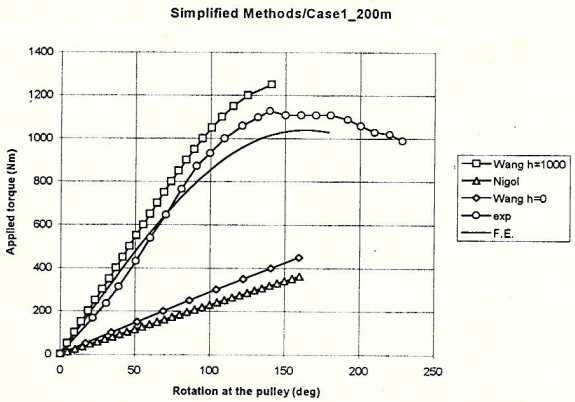

Fig. 5. Comparison of the experimental torque/rotation angle diagram with the simulated diagrams

Five curves are plotted on Fig. 5 : Nigol's simulation (equation 4), Wang's simulation for $h = 0$, Wang's simulation for $h = \infty$, the finite element simulation (explained with more details in the next section) and the experimental result (case1_200m). From this figure, it is clear that Nigol's theory is far from reality because no tension differences are assumed between subconductors during the torsional deformation of the bundle.

Wang's case $h = 0$ is also far from the experimental result because of the same reason. However, the slope of the curve is a little higher because Wang's theory takes into account the sag/span ratio of the line.

Wang's case $h = \infty$ is in harmony with the experimental results as well as the finite element simulation. This proves that the tension differences between subconductors which are induced by the yoke plates design, cannot be neglected in order to understand correctly the physical mechanism of bundle torsional stiffness.

The initial torsional stiffness (GJ *in* $Nm/\deg$) obtained with each simulated method and with the experimental case is given in Table 4. It corresponds to the linear part of the curves plotted in Fig. 5.

TABLE 4. INITIAL TORSIONAL STIFFNESS FOR THE DIFFERENT SIMULATED METHOD

	Nigol	Wang $h = 0$	Exp.	F.E.	Wang $h = \infty$
GJ	2.3	2.9	7.6	9.7	10.7

The finite element result remains in this table 27% bigger than the experimental result. In fact, the design of the spacers used at KANSAI EPCO is such that the rotation of the cables is free for some angles at the beginning of the bundle rotation and thus the intrinsic torsional stiffness of the cables doesn't contribute to the bundle torsional stiffness. Then, the cables are fixed in rotation and the intrinsic torsional stiffness participates again in the bundle torsional stiffness. This behaviour can also be observed on Fig. 5 where the slope of the experimental curve increases after the beginning of the rotation.

V. COMPARISON BETWEEN FIELD RESULTS AND FINITE ELEMENT SIMULATIONS

A. Presentation

The finite element modelisation of the tests that were realised at the KANSAI EPCO is presented below. These developments were introduced and managed in the software MECANO [6].

1) Cables

The four subconductors are represented by two nodes isoparametric cable elements with, for each node, four degrees of freedom, namely, three in translation and one in rotation around the tangent of the element. So that, for the cables, two kinds of deformation are taken into account : the longitudinal stretching and the torsion.

2) Spacers

The spacers are simulated by rigid bodies. Each spacer is connected with the cables in translation and in rotation. The connection in rotation between a spacer and the cables means that the intrinsic torsional stiffness of the conductors

contributes to the bundle torsional stiffness. To apply a torque on the bundle, one extra spacer (called the pulley) is used respectively at 50, 100 and 200 meters from the tower (Fig. 6).

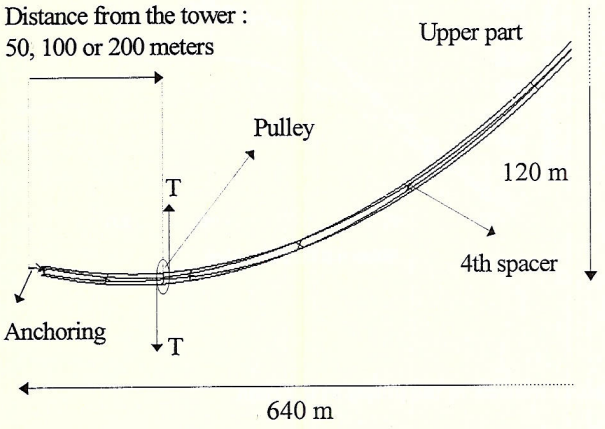

Fig. 6. Torsional bundle deformation induced by a torque applied at the different positions.

3) Forward anchoring

The modelisation of the anchoring is shown on Fig. 7.

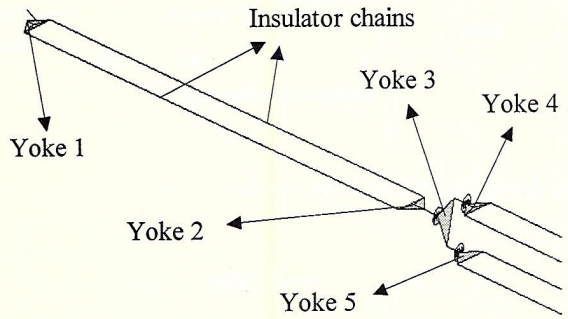

Fig. 7. Global view of the anchoring of the bundle on the tower

The different yoke elements are represented by rigid bodies, while the insulator chains are modelled by beam elements. Moreover, the yokes 2, 3, 4 and 5 are linked to each other thanks to rigid joint elements (Fig. 8).

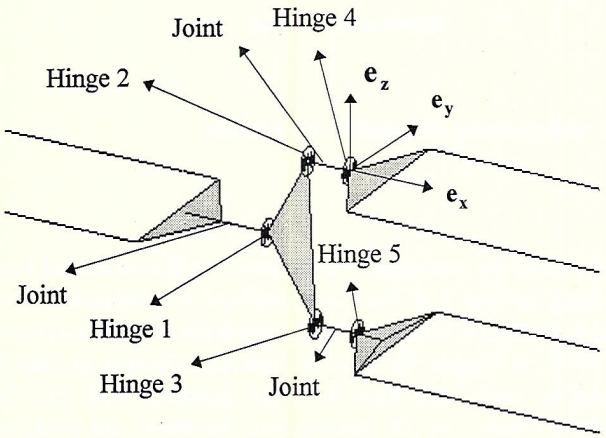

Fig. 8. Yoke plate arrangement for the quad bundle

As it is illustrated on Fig. 8, the connections between the yokes 3, 4 and 5 and the joint elements are realised thanks to hinge elements. In general, as it is explained on Fig. 8, a hinge element allows a relative rotation between a joint and a yoke in one direction $\mathbf{e}_x$, $\mathbf{e}_y$ or $\mathbf{e}_z$. With this representation of the anchoring, it becomes possible to simulate the different cases realised during the field tests.

In cases 1 and 2, the only free rotation is located in hinge 1 in the $\mathbf{e}_y$ direction. This situation was explained by the fact that for cases 1 and 2, a rod and a fixing plate were used to link together yoke plates 3, 4 and 5 (they are not drawn on Fig. 8).

The picture below shows this particular yoke plates arrangement.

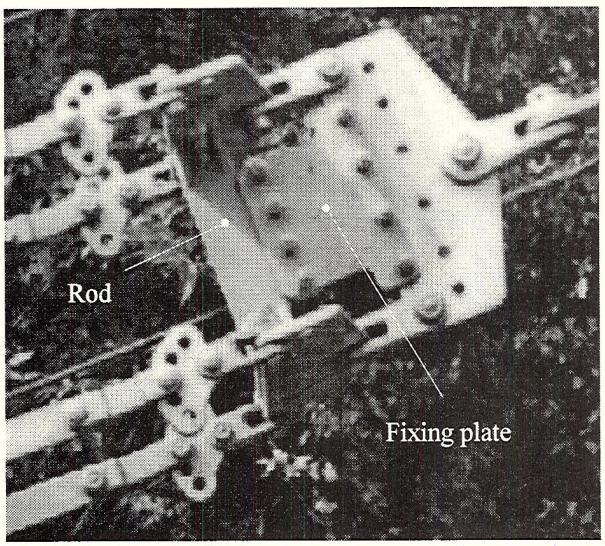

Fig. 9. Picture of the fixed yoke plates arrangement (case1 and case2)

The consequence of this is that yoke plates 3, 4 and 5 form a rigid body because no rotation is allowed in this arrangement.

On the other hand, in case 3, the rod and the fixing plate were removed so that five rotations are free, respectively located in hinge 1 in the $\mathbf{e}_y$ direction, hinge 2 and 3 also in the $\mathbf{e}_y$ direction and finally in hinge 4 and 5 in the $\mathbf{e}_z$ direction.

B. Results

The comparison with the experimental result case1_200m is presented together with the results of the simplified methods.

The other results of the comparison are presented on the next pages.

For every test, seven physical data were measured according to the rotation at the pulley where the torque is applied (Fig. 6). We have :

- the applied torque
- the tension in each subconductor (4 times)
- the rotation of the fourth spacer
- the rotation of the horizontal yoke in the $\mathbf{e}_x$ direction (= yoke 2 on Fig. 7)

Each of them is compared with the finite element result which is plotted with a full line and marked with the abbreviation "sim" in the legend while the experimental result is plotted with a dotted line and indicated with the abbreviation "exp" in the legend.

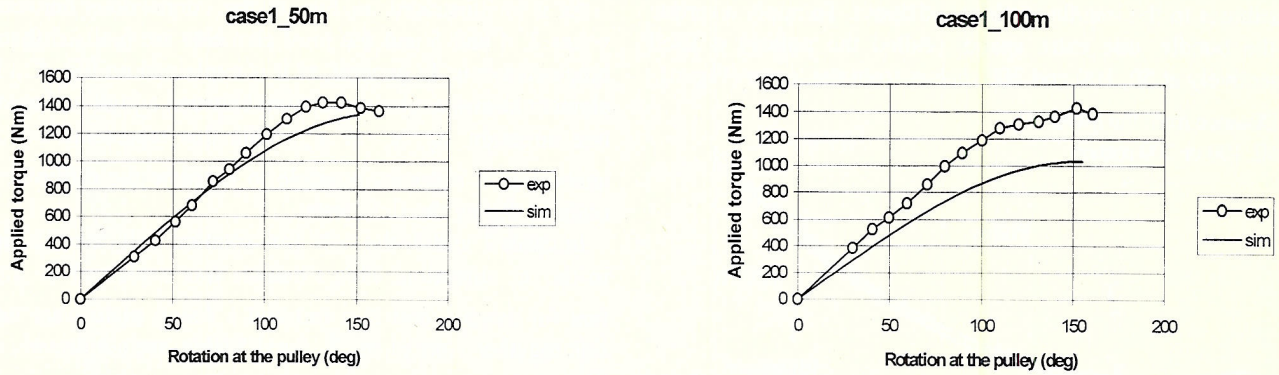

Fig. 10. Torque-rotation relationship for two different locations of the pulley in the span

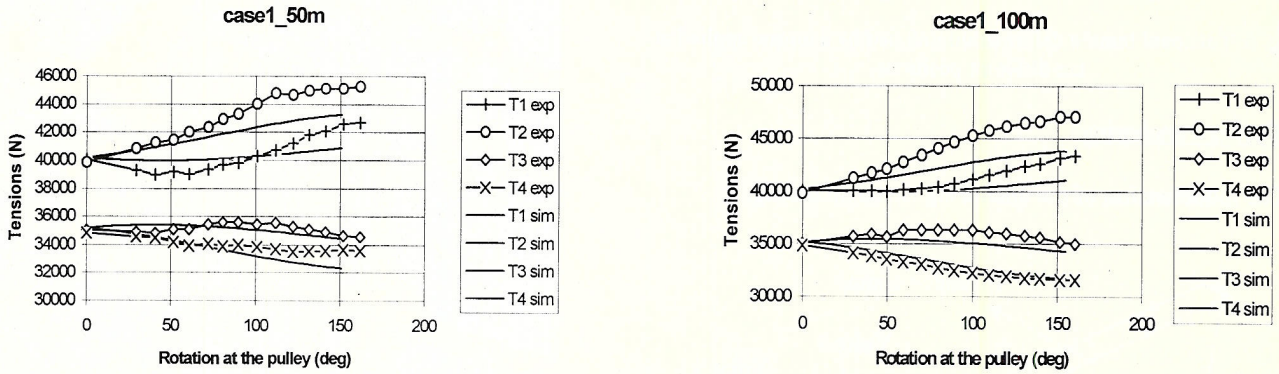

Fig. 11.. Tension variations in each subconductor during the rotation of the bundle

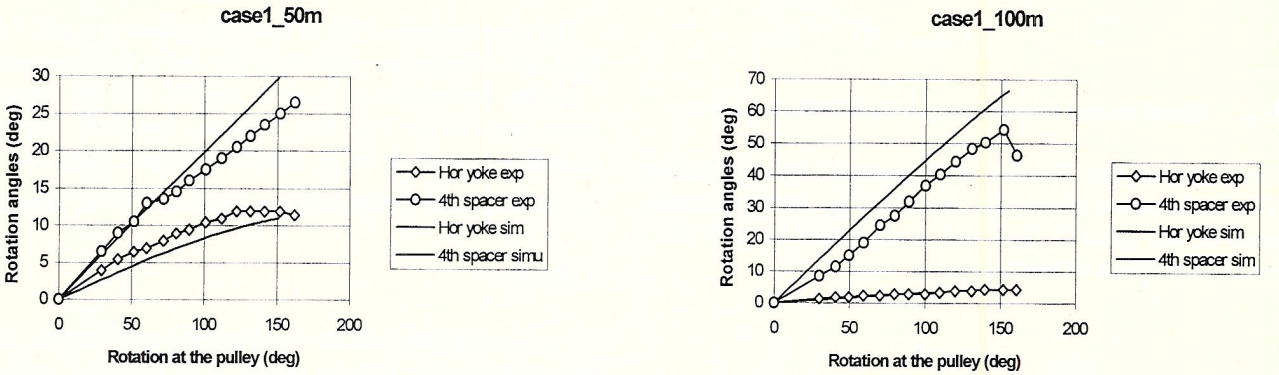

Fig. 12. Horizontal yoke plate and 4th inspan spacer rotation during the rotation of the bundle

1) Case1 (Mean tension = 37700 N, fixed yoke plates)

For the torque that is applied at 50 meters, the results of the finite elements are in harmony with the experimental results.

Concerning the torque applied at 100 meters, the simulated torque is far from the experimental result near the collapse.

However we can suspect some errors in the measured torque because in case 2 at the same distance, the maximum torque that is reached is almost the same when the mean initial tension is 10000 N bigger. So that the maximum torque in case 1 is probably lower and thus in better harmony with the finite element results. At 100 meters from the tower, the rotation of the fourth spacer is larger because this spacer is not far from the place where the torque is applied while the rotation of the horizontal yoke plate is smaller for the opposite reason.

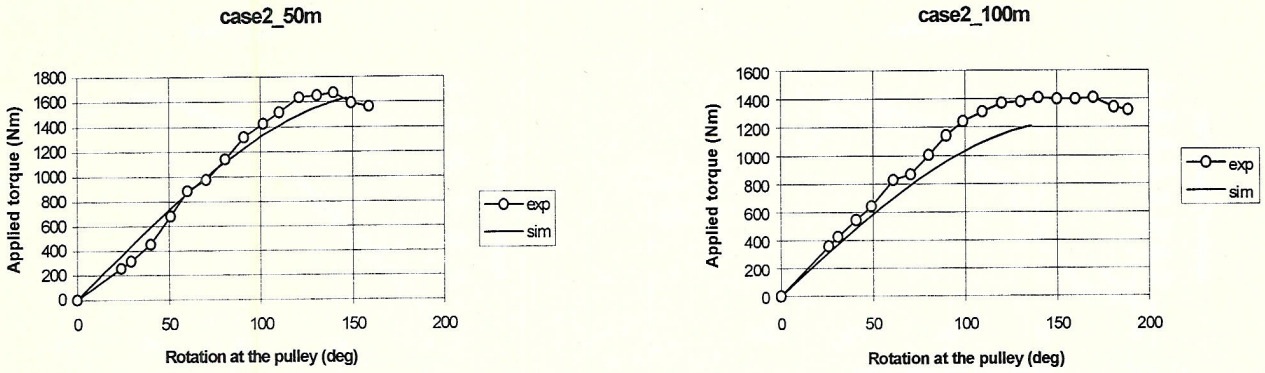

Fig. 13. Torque-rotation relationship for two different locations of the pulley in the span

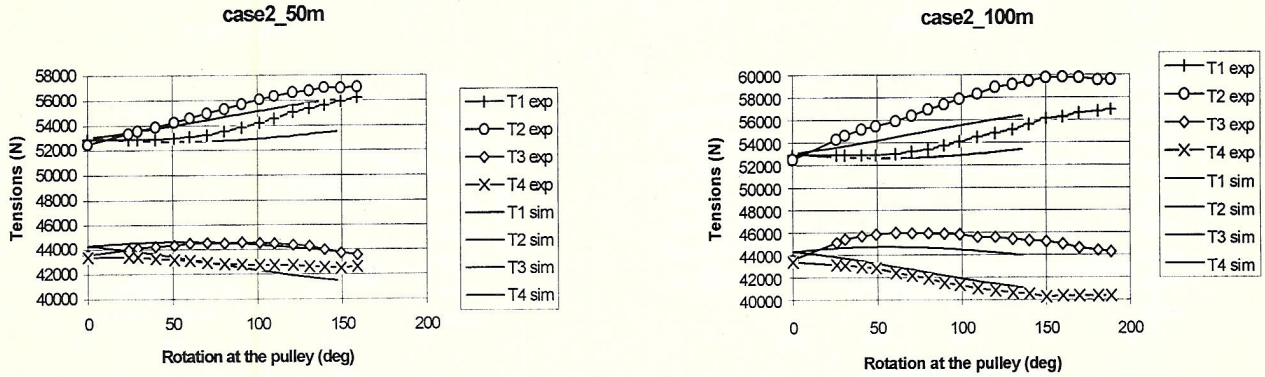

Fig. 14. Tension variations in each subconductor during the rotation of the bundle

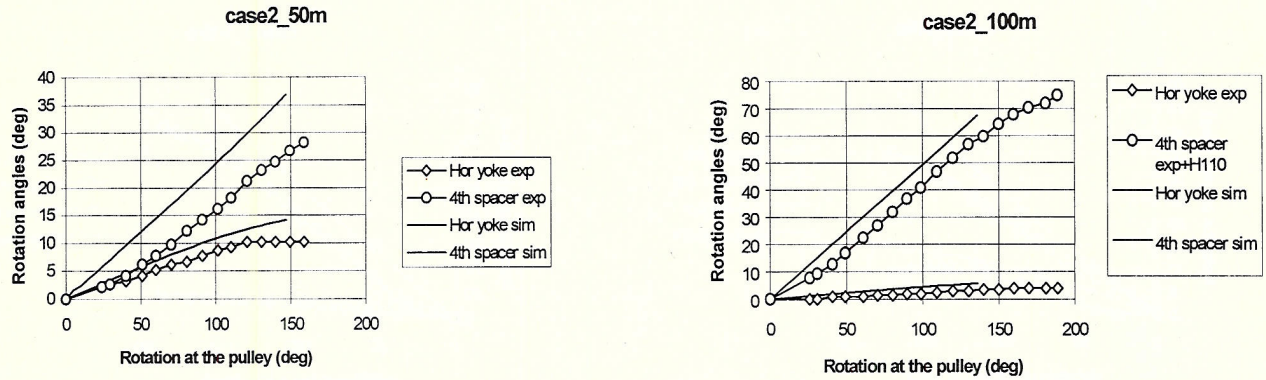

Fig. 15. Horizontal yoke plate and 4th inspan spacer rotation during the rotation of the bundle

2) Case 2 (Mean tension = 48650 N, fixed yoke plates)

Generally, the results of the finite elements are in good harmony with the experimental results excepted for the rotation angle of the fourth spacer at 50 meter.

The maximum torque which is reached, is higher than in case 1 because of the increase of the initial mean tension.

3) Case 3 (Mean tension = 46650 N, free yoke plates)

Again, generally, the finite element results are in good harmony with the experimental results.

The maxima torques which are reached, are just a little higher than in case 1 when the initial tension is 8000 N higher. The collapses appear for a bigger angle compared to case 1 and 2 (~160 ° in place of ~140°). Finally, the tension differences are smaller than in case 1 and 2.

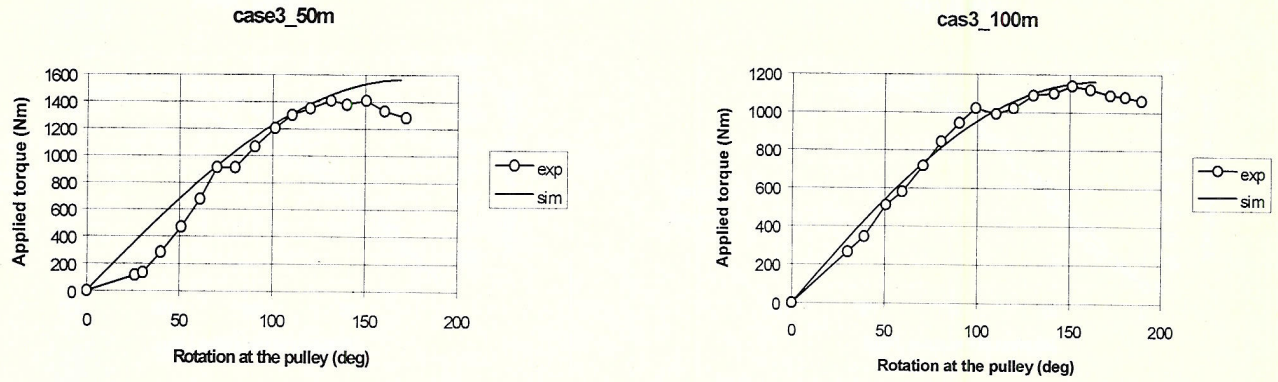

Fig. 16. Torque-rotation relationship for two different locations of the pulley in the span

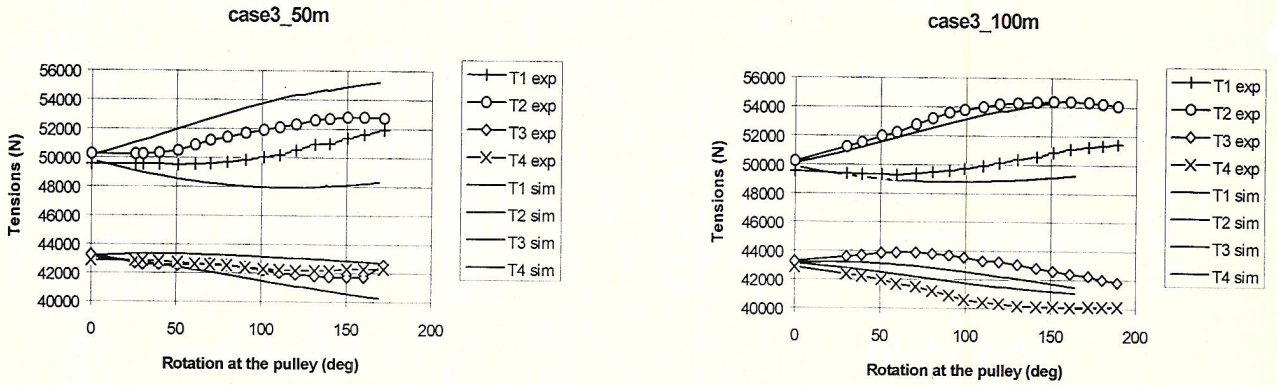

Fig. 17. Tension variations in each subconductor during the rotation of the bundle

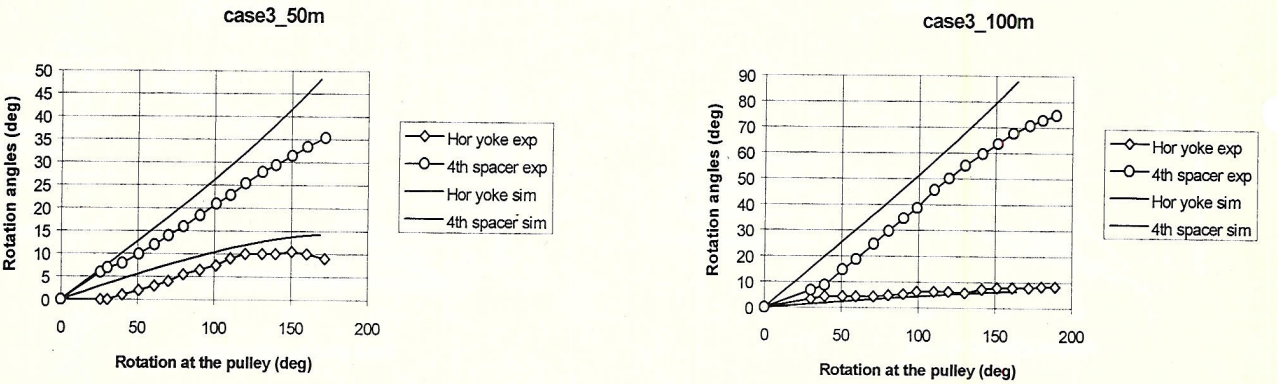

Fig. 18. Horizontal yoke plate and 4th inspan spacer rotation during the rotation of the bundle

All these facts find their origin in the design of the yoke plates which allows in this case some additional rotations so that the tension differences between subconductors are smaller.

4) Initial torsional stiffness

To summarize the different tested cases, Table 5 gives the initial torsional stiffness (GJ *in* $Nm/\deg$) of each of them, which is calcultated by the method of the finite elements.

TABLE 5. INITIAL TORSIONAL STIFFNESS FOR THE DIFFERENT SIMULATED CASES.

	Case1 50m	Case1 100m	Case2 50m	Case2 100m	Case3 50m	Case3 100m
GJ	12	9.8	15	12	14	11.2

In this table, we can see clearly that an increase in the initial tension (case 2 and case 3) induces an increase in the initial torsional stiffness. However, the increase in the initial torsional

stiffness in case 3 (17% at 50m and 14% at 100m) is smaller than in case 2 (25% at 50m and 22% at 100m) while the increase in the initial tension was nearly the same. This effect is explained by the yoke plate arrangement which is free in case 3.

VI. CONCLUSIONS

The different comparisons presented in this paper point clearly out the parameters that are involved in the physical mechanism of bundle torsional stiffness.

The most obvious of them are the mean initial tension of the bundle, the sag/span ratio of the line, the radius of the bundle and its variations inside the subspans during the torsional deformation, the number of subconductors and their intrinsic torsional stiffness.

Beside this, there is a set of parameters concerning the spacers. Indeed the number of attached spacers, their position in the bundle as well as the kind of fixation used between the spacers and the cables (gripped or rotating clamp) play an important role in the mechanism of bundle torsional stiffness.

Finally, the attachments of the bundle to anchoring towers by the use of yoke plates is also a key parameter of the bundle torsional stiffness. This point of the design influences the tension variations in the different subconductors during the torsional deformation of the bundle. It can leads, especially for transmission line with a small number of span to an important increase in the bundle torsional stiffness (more than 50% for a one span section like the tested quad bundle at the KANSAI EPCO).

Three theoretical methods were explained in the paper to underscore these different parameters.

Nigol's theory can only explain the bundle torsional stiffness mechanism for small rotations of the bundle and for specific attachment of subconductors. The tension in the different subconductor has to remain constant during the torsional deformation of the bundle. The latter condition is determined by the design of the yoke plates at the anchoring of the bundle on the towers. However, the influence of the design of the yoke plates decreases when the number of span in the section increases.

The theory which was recently developed by J. Wang, is valid for large rotations of the bundle since the model takes into account the sag/span ratio of the line and the variation of the radius of the bundle inside a subspan during the torsional deformation. But most of all, this theory can cover a wide range of situations thanks to the introduction of the design of the yoke plates in the calculation of the bundle torsional stiffness.

The finite elements method allows a complete description of the physical mechanism of bundle torsional stiffness.

This method has to be used to study some particular aspects which are not forecast by J. Wang's theory. It can concern a specific yoke plate design at the anchoring of the bundle on the tower, a sagging tension function of the subconductor, a span which is not level or any other aspect which can only be described by a finite elements discretisation.

VII. REFERENCES

[1] Nigol O., Clarke G. J., « Torsional Moment, Stiffness and Stability of Bundle Conductors, » *Ontario Hydro Research Division Report*, Report No.76-160-K, April 1976, pp. 1-9, fig. 61.

[2] Nigol O., Clarke G. J., Havard D. G., « Torsional Stability of Bundle Conductors, » *IEEE Transactions on PAS*, Vol. PAS-96, No.5, Sept./Oct. 1977, pp. 1666-1674.

[3] Nigol O., Buchan P. G., « Conductor Galloping, Part II - Torsional Mechanism, », *IEEE Transactions on PAS*, Vol. 100, No. 2, Feb. 1981, pp. 708-720.

[4] Dubois H., Lilien J. L. and Dal Maso F., « A New Theory for Frequencies Computation of Overhead Lines with Bundle conductors, » *Revue AIM Liège*, No.1/1991, pp. 45-62.

[5] Wang J., « Large Vibration of Overhead Electrical Lines : A Full 3-DOF Model for Galloping Studies, » *Ph.D. Thesis, Collection des Publications de la Faculté des Sciences Appliquées de l'Université de Liège*, No.151, 1996, pp. 1-227.

[6] MECANO, *Finite Element Software for Non-Linear Time Analysis,* Samtech, Liège, Belgium.

VIII. BIOGRAPHIES

R. Keutgen was born in Liège, Belgium, on October 18th, 1971. He received his degree in Mechanical Engineering from the University of Liège in 1994. He is currently a Ph.D. student at the same University. His research area concerns the study of single and bundle conductors galloping thanks to finite element simulations.

J. L. Lilien was born in Liège, Belgium, on May 24th, 1953. He received his degree in Electrical and Mechanical Engineering from the University of Liège in 1976. He received his Ph.D. from the same University in 1984. He is presently a professor at the same University, Dept. Of Transmission and Distribution of Electrical Energy. His main activity is based on the effects of short-circuit mechanical effects and overhead lines vibrations (galloping). He is the chairman of the CIGRE task force on the effects of short-circuit in substation (belonging to WG 23-11). He is also expert of the CIGRE task force on galloping (belonging to WG 22-11). He has published over 60 technical papers and participated to many symposia and international conferences. He received the international prize « George Montefiore » in 1986.

T. Yukino works at the Kansai Electric Power Co, Osaka, Japan. He is a specialist inside his company of the galloping problems. He has a widely experience on mechanical problems of overhead transmission lines. In 1995, he managed the artificial torsional tests that were carried out on the full-scale long dead-end span at Yamasaki Test centre.

DISCUSSION

YOSHIHIKO. OTA, Nippon Katan Co., Ltd.
Hirakata Japan:

When a structure analysis is carried out by using a finite elements simulation, it is very important to guarantee the validity of calculating method, that shall be confarmed whether a set element's function acts as like as an equipment. For the above reason, the consideration of this paper is one of the most valuable results.

In Nippon Katan, we have considered a stiffness to aim at a structure of insulator assembly as explained below. So, we hope that the authers may consider the our experiment.

Generally, torsional characteristic of multi bundled conductor is very important fuctor to design an optimum disposition of inspan spacer and to analyze a galloping phenomena.

This torsional characteristic is determined by calculating a function comporsed with the kind of conductor, the number of conductor, diameter of bundle, tension in conductor, span length, different of ancoring level, subspan length and the structure of insulator assembly in addition to them.

The optimization of inspan spacer disposition is designed aganst both a dynamic stability and a withstand torsioning.

This characteristic is affected from different of insulator asembly's structure(fixed type, free type of york).

In the case of fixed type, maximum resisting torsional morment becomes large because of it's large torsional stiffness and minimum one become small.

On the contrary, against the free type, the maximum resisting torsional morment becomes smaller and minimum one becomes larger.

On an analysis of galloping phenomena, it is suggested that a resonant between torsional period and inplane vibration period make a conductor locus increase. The torsional stiffness of insulator assembly is one of the important factors for calculating a torsional period.

The design formula to calculate a torsional characteristic has been considered with a yoke structual coefficient to be concerned with the torsional stiffness of the insulator assembly. The value of this yoke structual coefficient for a tension strings is obtained by calculating the formula(1) led from a full scale experimental data. For suspention strings, another formula has been established too.

$$Kt = 2.77\sqrt{h}/a \qquad (1)$$

Kt: yoke structual coefficient of insulator assembly for tension strings
h : offset of yoke plate (m)
a : diameter of the bundle (m)

We have carried out the fullscale vibration test for comparison of an experimental torsional period with calculated one. The result is shown in Table 1.

Table 1. Comparison of vibration period (sec)

kind of assembly structure		free type	fixed type	
torsional period	1roop	1.42(1.59)	1.09(0.94)	Twin conductor of ACSR 410mm2
	2roop	0.78(0.80)	0.77(0.76)	span=80m
	3roop	0.56(0.53)	0.55(0.51)	Tension=11.8TN per conductor
in-plane vibration period	1roop	1.02	1.02	( ):calculated
	2roop	0.95	1.00	
	3roop	0.63	0.60	

In Table 1, it is clear that the torsional period of free type of yoke is diffferent from fixed type of yoke plate on one roop. In this case, the yoke structual coefficient is obtained the value of 0.7.

The calculated periods are closely agreement with the experiment one.

Manuscript received February 27, 1998.

R. Keutgen, J.L. Lilien, University of Liège, Liège, Belgium and T. Yukino, Kansai Electric Power Company, Japan:

The authors would like to congratulate M. OTA for his very detailed comments and its useful participation on the discussion on our paper on torsional stiffness.

We would like first to refer to another paper published 1991, unfortunately only published in a local Journal in Belgium [1] where it is detailed a torsional stiffness theory including yoke plate offset. In that paper the interaction between yoke plate and torsional frequencies is clearly pointed out and the authors went out with a yoke factor effect, which for a twin horizontal conductor gives

$$\frac{1}{K_\theta} = \frac{a^2}{2hT} + \frac{L}{EA} \qquad (0.1)$$

Where, as for the discusser, a is the subconductor separation, h is yoke plate offset. Moreover some other datas are taken into account, like subconductor tension (T) and extensional stiffness of the span (E, the elasticity modulus, A, the cross section and L the span length, coupled to give EA/L)

Taken this coefficient into account to evaluate another one (neglecting intrinsic torsional stiffness)

$$M_\theta = \frac{8w^2 K_\theta L^3}{\pi^4 T^3} \qquad (0.2)$$

where w is the subconductor weight.

This factor M_θ is generally in the range 0 to 10, often close to 3.

We have access to torsional frequency which is approximately (neglecting intrinsic torsional stiffness)

$$f_\theta = \Omega_\theta \sqrt{1 + 2M_\theta} \qquad (0.3)$$

where

$$\Omega_\theta = \frac{\pi}{L}\sqrt{\frac{T}{m}} \qquad (0.4)$$

with m the subconductor mass per unit length.

If the yoke plate is fully rigid, means h equal to infinity, we just replace K_θ by EA/L, giving a strong increase of torsional frequency, compared to basic one.

If the yoke plate is called « free », h equal to zero and M_θ has no influence on frequency.

In any case mainly the first frequency is changed, the even ones (2, 4, ...) are unchanged and the following odd ones (3, 5, ..)) are very slightly affected.

Let's remember that yoke plate effect is due to its impact on tension variations between subconductors during bundle rotation.

If we would like to compare this formulation with discusser's one, we have to imagine a small yoke plate offset, for which K_θ is equal to the first term only in (0.1), thus giving appropriate M_θ using (0.2), then using (0.3) by neglecting 1 face to $2M_\theta$. Then the torsional frequency is proportional to the square root of M_θ, means the square root of h, divided by a, the subconductor separation, exactly the same as discusser's one.

Of course, if finite element method is used all these effects are « naturally » taken into account in the model, without any specific modelisation, because actual geommetry is used in the model. The former discussion clearly points out the absolute necessity to include more or less exact yoke plate assembly into account.

The example given by the discusser is interesting to clearly point out that the first frequency (period) of torsional movement could be close to second one, sometimes even higher (lower). This is fundamental to clearly understand how bundle could gallop on two loops in dead-end spans, in some cases (flutter type galloping). This is also fundamental to imagine anti-galloping design based on suspension yoke plate assembly, as explained in the paper of J. Wang [2].

It is difficult to reproduce discusser's case because of many missing datas, like subconductor separation, yoke plate offset and uncompatible datas (the second vertical frequency is not influenced by yoke plate and can be obtained very easily by taut spring formula, which canot be verified in discusser's case. May we kindly ask him to contact author by e-mail at lilien@montefiore.ulg.ac.be).

In any case, the influence of the yoke plate design on the first torsional frequency is evident if we look at Table 1 of Y. Ota's discussion. This is a very important fact because it means that a detuning effect between the torsional frequency and the vertical frequency can be obtained with a well suited yoke plate design.

We would like now to confirm the importance of such yoke plate design on the galloping phenomenon. To do this, we have realised finite element simulations with a 2-span twin bundle conductors as depicted on Fig. 1. Two different cases were tested. In the first case, the subconductors are fixed at the ends of the line section, this corresponds to a yoke offset $h \to \infty$, while in the second case a yoke plate is used for the fixation with an offset $h \to 0$.

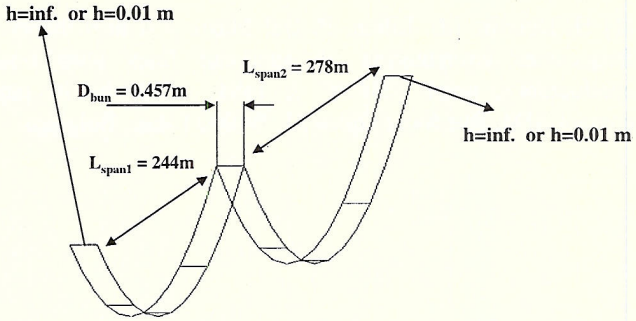

Fig. 1. Two configurations of a 2-span twin bundle conductors.

The first tuned eigenmodes of these two cases are given in Table 1.

Tuned eigenmodes	
Case 1, $h \to \infty$	**Case 2, $h \to 0$**
V1 (Up-Down) 0.29 Hz	V2 (Span 2) 0.54 Hz
T1 (Up-Down) 0.30 Hz	T2 (Span 2) 0.55 Hz
	V2 (Span 1) 0.61 Hz
	T2 (Span 1) 0.63 Hz

Table 1. First tuned eigenmodes of the two configurations

In case 2, the tuning between the vertical (« V » in Table 1) and the torsional frequency (« T » in Table 1) appears for a higher frequency. This can be explained by the fact that when $h \to 0$, there is no tension variations between subconductors when the bundle rotates so that coupling between spans is avoided in torsion and thus the up-down mode in torsion doesn't exist.

We have simulated these two cases for different wind speed in galloping conditions. The corresponding amplitudes are plotted on the graphic of Fig. 2.

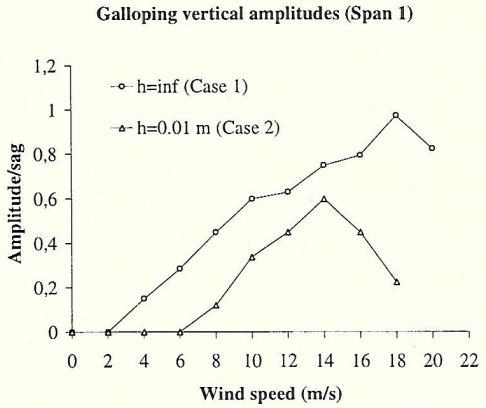

Fig. 2. Galloping amplitudes

These results show clearly that the yoke plate design influences the detuning between vertical and torsional modes and hence the amplitude of the flutter galloping vibration.

[1] H. Dubois, J.L. Lilien, P. Dal Maso, « A new theory for frequencies computation of overhead lines with bundle conductors », *revue AIM N° 1*, 1991, to obtain the paper, contact AIM, Rue Saint Gilles 31, B4000 Liège, Belgium.

[2] J. Wang, J.L. Lilien, « A new theory for torsional stiffness of multi-span bundle overhead transmission lines », *IEEE Winter meeting*, paper PE-217-PWRD-0-11-1997, Tampa, USA, February 1998. Accepted for publication in the transactions on power systems.